Effect of Solvent Casting on Reduced Entanglement Density in Thin Films Studied by Ellipsometry and Neutron Reflection

Bryan B. Sauer* and David J. Walsh

E. I. DuPont de Nemours and Company, Inc., Central Research and Development, Experimental Station, Wilmington, Delaware 19880-0356

*Received June 18, 1993; Revised Manuscript Received October 15, 1993**

ABSTRACT: Neutron reflection (NR) and spectroscopic ellipsometry (SE) were used for the investigation of the interfaces between films of poly(vinyl methyl ether) (PVME, glass transition temperature (T_g) = -31 °C) and polystyrene (PS, $T_g \sim 105$ °C). The transport of PVME into PS at temperatures below the glass transition of PS was highly non-Fickian. The linear dependence of the front propagation with time, along with the high activation energy for transport indicates some similarities to classical case II transport of solvent into polymer glasses. The variation of PVME transport rate with PS molecular weight (MW) illustrates one significant difference as compared to classical case II transport. The strong dependence of PVME transport rate on PS MW is attributed to the MW dependence of the rate of swelling and dissolution of PS in the swollen front region. It was also found that the transport rate (front velocity) of PVME into PS depended strongly on the temperature and time of preannealing of the single spin coated PS layer. Preannealing at temperatures well above T_g for higher MW PS films was necessary. Birefringence measurements on PS films proved that internal stress was not a factor. A systematic MW study indicated that the major factor was the reduced entanglement density due to spinning of PS films from solution.

Introduction

Polarized optical reflection methods such as single wavelength ellipsometry are useful for the study of polymer/polymer interfaces[1-3] because of the high resolution. The analysis and interpretation are generally difficult because only two ellipsometric parameters are measured. The situation is improved by using frequency scanning ellipsometry (or spectroscopic ellipsometry) (SE).[4] For SE two ellipsometric parameters are measured at each wavelength, and the extra information allows one to model complicated interfaces and multilayer systems.[4] Only recently has SE been applied to polymer/polymer interfaces.[5,6] Compared to the study of inorganic/inorganic or organic/inorganic interfaces, one is limited to a certain extent because of the lower resolution in the case of the small refractive index differences encountered between typical polymers. The precision in the interfacial thicknesses determination for polymers is still high and is generally on the order of 1-5 nm for SE, depending on the refractive index differences. Even though the resolution of SE is decreased in cases of low contrast, the interfaces between polymers are usually broad so ellipsometry is still quite useful. Deuteration is not necessary, making SE quite versatile for systems where synthesis of deuterated polymers is not an option. SE is also superior to most other techniques for monitoring changes in thicknesses in the case of thick layer systems. For example, it can be readily used if both layers are on the order of 500 nm or greater, whereas techniques such as neutron reflection (NR) and other destructive techniques cannot easily access these dimensions. NR is very precise and accurate for narrow interfaces,[7] but loses sensitivity in terms of quantifying dimensions of interfaces broader than tens of nanometers. This loss in sensitivity for broad interfaces becomes worse if the interfaces are asymmetric.[6]

Previously, we had chosen the miscible pair poly(vinyl methyl ether) (PVME, T_g = -31 °C) and polystyrene (PS, $T_g \sim 105$ °C) because it was believed that it would be an ideal model system with which one could compare the capabilities of a relatively well established technique such as NR, versus SE.[6] Because the films were thin, the temperature was lowered to well below the T_g of PS to slow down interdiffusion, and it was discovered that transport was highly non-Fickian.[6] Subsequent experiments[8,9] verified this non-Fickian transport for PS/PVME and also showed that the ATR-FTIR technique[8] could be used to study interdiffusion both above and below the T_g of PS, although details of the interfacial profile could not be resolved by that technique. Detailed modeling of the transport processes allowed the determination of the relative contribution of Fickian and non-Fickian processes as a function of temperature.[8]

Interdiffusion between other miscible polymers at temperatures below the T_g of one of the components, has also been studied by forward recoil spectroscopy (FRES), which is a direct profiling technique.[10] For the miscible pair PS/poly(xylenyl ether) (PXE), PXE (T_g = 217 °C) was the high T_g component, and the evolution of the PS penetration front into PXE was studied below its T_g. Fickian dissolution of PXE into the PS phase was monitored by the direct profiling technique.[10] Because of the low volume fractions involved, a comparable Fickian dissolution profile of PS in the PVME phase could not be studied by SE,[6] although other evidence indicates that it most likely exists.

A schematic of a typical 75 °C non-Fickian transport process as determined by SE is given in Figure 1, illustrating the evolution of the interfaces and the partial dissolution of PS into the PVME phase. As will be discussed later, Figure 1 illustrates a typical case where the PVME/PS interface broadens but stays symmetric. This is in direct contrast to case II solvent penetration into a polymer glass, where the penetration front is highly asymmetric because negligible polymer dissolution occurs.[11-13] In this case, the asymmetric penetration front consists of 10% to 20% solvent (i.e., 10% to 20% total swelling of the glassy polymer), whereas the PS swollen by PVME in the "front region" swells indefinitely[6] because it eventually dissolves.

A related situation is polymer dissolution by solvent where elastic stresses of swelling in addition to polymer dissolution effects have been considered theoretically.[14,15]

* Abstract published in *Advance ACS Abstracts*, December 15, 1993.

0024-9297/94/2227-0432$04.50/0

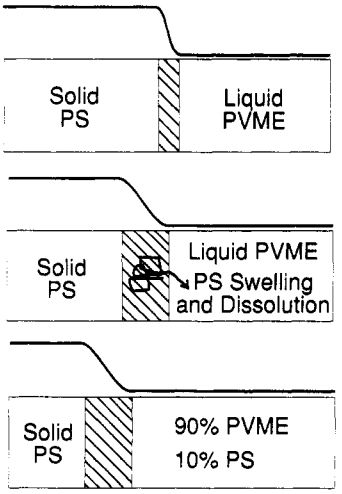

Figure 1. Schematic of the evolution of PVME transport into glassy PS at ~75 °C. The evolution of symmetric concentration profiles of PS normal to the plane of the films is also shown. The top indicates the sharp symmetric interface for the as prepared bilayer. The middle schematic indicates a broadening of the interface with a small decrease in PS layer thickness. The bottom indicates that the PVME is penetrating and dissolving away part of the PS layer, leading to a further decrease in the PS layer thickness and an increase of PS in the PVME phase. The plot indicates 10% PS in the PVME phase as an example of an intermediate stage, but generally, PS will indefinitely mix in the PVME phase depending on the starting layer thicknesses.

These theories do not address the mechanical relaxation effects at the boundary between swollen and unswollen polymer glass, which are the key factors in case II solvent transport and are also quite important with PVME/PS. At this time, there is little hope for a quantitative theoretical description of the complicated dependence with MW. A rigorous continuum theormodynamical theory[16] for low MW solvent transport in polymers is available which adequately describes case II behavior, as has been shown by comparison with experiment.[17] Direct application of this theory is inappropriate for films of PS/PVME, since the effects of chain entanglement and MW are difficult to incorporate into a continuum theory.

Classical case II solvent front velocities are relatively independent of the polymer glass MW because dissolution of the polymer is not a factor, only mechanical relaxations and local friction effects on a length scale much smaller than the chain dimensions.[11,12] With a high MW penetrant such as PVME, mechanical relaxation effects in the front region between swollen and unswollen PS are also important and give rise to the highly non-Fickian behavior.[6,8,9] We will show below that an important distinction from classical case II transport is the strong influence of PS MW on the PVME penetration rate. The results suggest that because of the large "penetrant" (PVME) size and slow front velocities, the MW dependent swelling and dissolution rates of PS dramatically influence the transport rate. The other major effect considered here is the extent of relaxation toward an equilibrium entanglement state in the solvent cast PS films, and how this affects subsequent PVME transport

Experimental Section

Materials and Sample Preparation. The bilayers of PVME and PS were prepared using a three step procedure. First, PS in xylene was spin coated onto glass. Next, the PS films were "preannealed" in an oven with a N_2 purge, generally at $T \geq T_g$. Finally, the PVME layer was spin coated directly on the PS layer, from *n*-butanol which is a nonsolvent for PS.

Originally, preannealings were performed on the single spin coated PS layers close to T_g in order to remove the spinning solvent (xylene) and to relax orientation. Both of these were successfully accomplished at T_g (see birefringence data below). On the other hand, the temperature and extent of preannealing turned out to be quite important because of the effect of reduced entanglement density in the PS layer on the rate of PVME interdiffusion. For example, with higher MW PS preannealing at temperatures well above T_g was necessary to fully equilibrate the PS chains.

The PVME was obtained from Scientific Polymer Products and had a M_w of 100k with M_w/M_n = 2.3 determined by gel permeation chromatography (GPC). Part of this sample was reprecipitated in warm water. GPC indicated that most of the low MW fraction was removed. Overall, the M_w increased to 120k and the dispersity decreased to $M_w/M_n \sim 1.8$. Only very small differences were seen for these two PVME samples in terms of the experiments reported here, so the unpurified M_w = 100k PVME sample was used in most cases. Water or other retained solvents in the PVME layer were found not to influence the results presented here. The bilayers were annealed in an oven (air) between 20 and 100 °C in order to examine interdiffusion. Before spin coating the PVME layer, the PS layer thickness was determined by SE in order to determine the quality of the film and also to help in making the initial guesses for the film thicknesses when fitting the bilayer SE data.

Narrow molecular weight distribution polystyrenes (PS) were used for all studies. For M_w = 10k, 100k, 1000k and 20000k PS, concentrations in xylene of approximately 10%, 6%, 2%, and 0.2% were used for spinning speeds of ~1000 rpm. All except the 20000k sample were filtered with 0.45-μm PTFE filters. In cases where both SE and NR data were needed for the same sample, large glass optical flats (manufactured as uncoated Pyrex mirrors, Melles Griot, 5-cm-diameter Pyrex borosilicate glass, smooth to $\lambda/10$) were used for spin coating. For SE, these large glass flats were not always needed, so in some cases smaller and thinner glass flats were used. No systematic differences were seen in interdiffusion results for starting thicknesses of PS and PVME between 150 and 700 nm.

Methods. The NR experiments were performed at Argonne National Laboratories using the pulsed source and the POSY II spectrometer with a time-of-flight detector. Data for each sample as a function of neutron momentum ($q = 2\pi(\sin\theta)/\lambda$, where θ is the grazing incident angle and λ is the wavelength) were obtained by signal averaging for 1–4 h. The scattering length density determined from the data for the PVME layer was b/V = 1.6-($\pm$0.1) $\times 10^{-10}$ cm^{-2} for PVME, in good agreement with the value calculated on the basis of chemical composition. The value of b/V for deuterated PS was 6.5($\pm$0.05) $\times 10^{-10}$ cm^{-2}. In terms of the simulations, the interfacial dimensions will be presented in terms of linear gradient profiles, i.e., the error function width $\langle z^2\rangle^{1/2}$ multiplied by a factor of 2.[6,18]

The spectroscopic ellipsometer and analysis software were supplied by Sopra (Distributed by Aries, Concord, MA 01742). Generally, 15–30 data points at values of λ between 300 and 650 nm were obtained, taking less than ~10 min. These were sufficient for modeling of the two layers and the polymer/polymer interface. To model the SE data, a refractive index (n) "basis file" as a function of λ must be generated for each polymer and the substrate. Values of $n(\lambda)$ for the polymer are readily determined via ellipsometry, as was discussed previously.[6] The refractive index of PS ranges from n = 1.695 at λ = 300 nm to n = 1.591 at λ = 600 nm. The two ellipsometric angles, the amplitude attenuation (ψ), and the phase shift (Δ) between the in-plane and out-of-plane polarized light, were obtained as a function of λ for each sample. Refractive indices were also determined from the measured ψ and Δ for PVME which was spin coated on silicon, and varied from n = 1.504 at λ = 300 nm to n = 1.465 at λ = 600 nm. Regression on ψ and Δ spectra, simultaneously, was performed using three to five parameters (two film thicknesses and steps of various concentrations as crude models of the interface). Some discussion of simulated polymer interface profiles to estimate the sensitivity of SE to various profile shapes has been given.[6]

For film birefringence measurements, the thickness (t) and refractive indices (n) were measured using a Metricon PC-2000 Prism Coupler manufactured by Metricon Co., Penington, NJ. The coupler was used for waveguide propagation modes in the

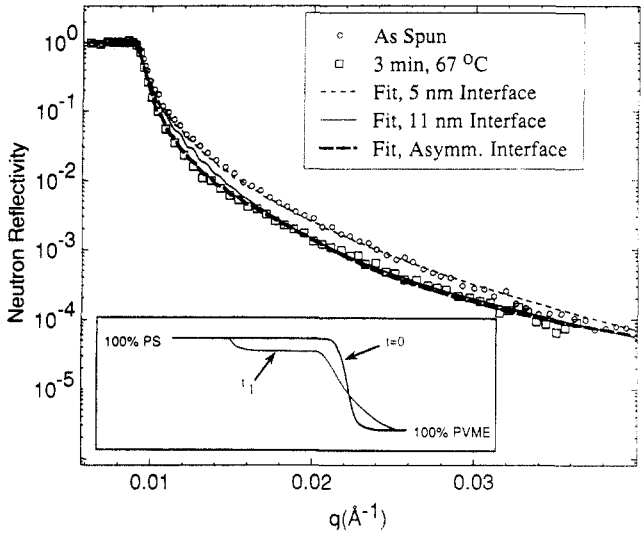

Figure 2. Neutron reflectivity vs neutron momentum (q) for 100k PMVE/1000k deuterated PS before and after a 3-min anneal at 67 °C. The indicated fits show that the interface profile is symmetric for the as spun bilayer and asymmetric after annealing at 67 °C. Inset: Schematic of the concentration profiles normal to the plane of the films (see text). These profiles were used to generate the fits for the as spun (t = 0) and 3-min annealed (t_1) reflectivity data. The profile after annealing (t_1) illustrates the broadening and also the asymmetric penetration front consisting of a low PVME volume fraction extending into the PS layer.

PS spin coated films. By detecting the propagation modes, t and the refractive indices could be calculated. To distinguish between the in plane ($n_\parallel$) and out-of-plane ($n_\perp$) refractive indices, transverse electric (TE) propagation modes were used for $n_\parallel$, and transverse magnetic (TM) propagation modes were applied to determine $n_\perp$ using the previously measured value of $n_\parallel$. Laser wavelengths for the waveguide measurements were 633 and 1300 nm.

Results

The first part of this section will be devoted to the examination of asymmetric profiles by NR and SE. In all cases, these were only observed when incompletely relaxed high MW PS layers were studied. The rest of the report will concern determination of macroscopic PVME penetration front velocities by SE in order to understand the effects of the PS MW and incomplete relaxation in the PS layers.

Asymmetric Interfacial Profiles. During the course of this study it was found that higher PS molecular weights accentuated the broad asymmetric interfaces consisting of a penetration front consisting of a low PVME volume fraction extending into the PS layer (inset, Figure 2). Neutron reflectivity data are given in Figure 2 for a 320-nm film of PVME on top of a 290-nm-thick film of 1000k deuterated PS (dPS). The 30-min preannealing at 110 °C for the 1000k dPS layer will be shown later to be insufficient in terms of fully relaxing the 1000k PS. The incomplete relaxation exaggerates the asymmetric profiles. Before annealing, the as spun bilayer has an interface that is symmetric and sharp with a dimension of 5 ± 0.1 nm. After annealing for 3 min at 67 °C, the only profile found which would adequately fit the data, was an asymmetric one with a 9-nm linear gradient interface combined with a 15% PVME asymmetric tail extending 15 ± 4 nm into the PS layer (inset, Figure 2). No reasonable fit with a symmetric profile could be found. This asymmetric profile is not a unique solution. For example, the inset of Figure 2 suggests that the 15-nm asymmetric tail is constant in concentration, but the data do not have sufficient sensitivity to uniquely determine this. Equivalent fits could be made with the concentration varying continuously over this 15-nm dimension, as long as the PVME volume fraction was kept small. This insensitivity is because the NR data are mostly sensitive to the maximum gradients in concentration and are rather insensitive to fine details of the asymmetric tail. The annealing conditions for the data in Figure 2 were chosen in order to study the early stages of interdiffusion, before the interface became too broad because of the known limitations of NR in the cases of broad interfaces.[6]

Table 1. Simulation of Ellipsometry Data To Obtain an Asymmetric Profile for Interdiffusion at 75 °C, PVME (100k)/Deuterated PS (1000k)

time, min	thickness, nm: PVME	interface no. 1[a]	interface no. 2[a]	DPS	χ^2
0	318 (100% PVME[b])	2.4	0	275	0.0069
1	321 (100% PVME[b])	15	0	262	0.0051
6	350 (97% PVME[b])	13.6	57	181	0.0125
9	368 (96% PVME[b])	31.5	74	132	0.0066
13	397 (88% PVME[b])	34.8	81	92	0.0076
17	430 (80% PVME[b])	26	90	55	0.0065

[a] Interface no. 1 is composed of 55% PVME/45% PS and interface no. 2 is 14% PVME/86% PS. These two blocks are used as a crude representation of the actual asymmetric interface (see text). [b] Determination of the refractive index of the PVME "layer" by ellipsometry gives these compositions directly.

Whereas NR is only useful for the early stages of interface broadening for this system, SE can be used to monitor the entire process because of its sensitivity to very broad interfaces. The preannealing conditions for the single 1000k PS film were the same as above, i.e., the PS is not fully relaxed. After spinning PVME on the PS layer, the interface was found to be sharp for the as prepared sample (Table 1). Upon annealing at 75 °C the interface becomes very broad and asymmetric and reaches a total of ~110 nm. Table 1 indicates that a steady state dimension of about 80 nm is attained after ~9 min for the asymmetric front consisting of 14% PVME. This is 2–3 times as large as those determined in the previous report with 100k PS.[6] Higher MWs lead to broader interfaces because of the slower swelling and dissolution rates of PS into the PVME phase. The better agreement of the fits generated by the asymmetric profiles as opposed to the symmetric profile, are judged by the χ^2 values obtained from the regression fit of the SE data (Table 1). The improvement in the χ^2 values was typically 15%. As was the case with NR, SE is not sensitive enough to determine the exact shape of the asymmetric tail of the low volume fraction of PVME extending into the PS. We assumed step-function profiles for all fits, as is indicated in Table 1. Direct profiling techniques such as FRES would be useful for further quantification of the shape of the interfaces.

The PVME layer composition is determined by modeling the SE data in terms of the layer refractive indices. It is found that the PS concentration in the PVME layer increases with time (Table 1), consistent with a decrease in the PS layer thickness. The precision is better than a few percent. The refractive index of the PS layer is found to remain constant at the value for pure PS. Very little information on the actual shape of the PS dissolution profile into the PVME phase is obtained. The concentration gradients are quite small and SE is not sensitive enought to detect them. Details of this Fickian dissolution process have been studied by direct profiling techniques in a similar system.[10]

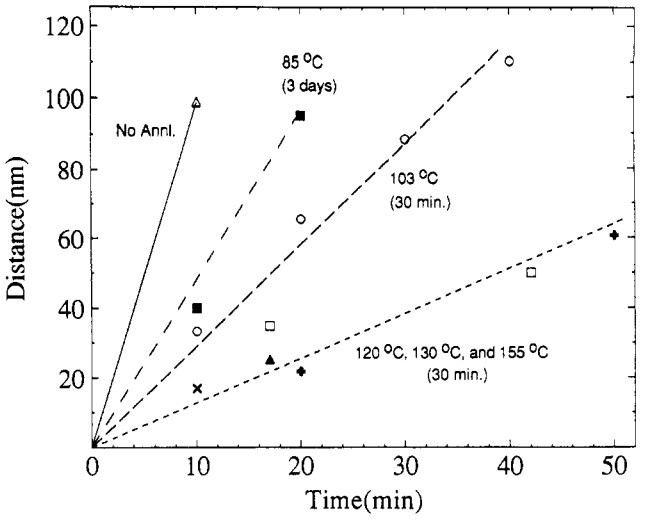

Figure 3. Penetration distance of PVME into PS as indicated by a decrease in the 100k PS layer thickness at interdiffusion temperatures of 75 °C. Preannealing of the PS layer for the indicated times and temperatures was performed in N_2.

Effect of Incomplete PS Relaxation on Front Velocity. The majority of this report will deal with observations of the variation in the PVME front position as a function of sample history and interdiffusion temperature. Asymmetric profiles were not observed for the PS/PVME bilayer if the PS films were "completely relaxed". The interfaces for completely relaxed PS films are symmetric and are on the order of 10 nm for low MW PS and 40 nm for high MW PS. Generally, the variations in front position are much larger than the interface dimensions, so the exact shapes of the interfaces are not important for the results presented below.

Figure 3 shows an example of the front position for 100k PS/100k PVME at an interdiffusion temperature of 75 °C. The slope of the lines gives the PVME front velocities, V. There is about a factor of 10 decrease in V for the sample which was not preannealed, as compared to the samples preannealed at 120 °C or higher. Preannealing at $T \geq 120$ °C gives rise to a limiting value of V, while preannealing at the T_g (~105 °C) of 100k PS leads to values much lower than this limit. All data in terms of the front velocity of PVME into the PS layer are consistent with a linear dependence with time (Figure 3). None of our data for bilayers annealed below the T_g of PS can be modeled with a Fickian ($t^{1/2}$) dependence. In addition, no skin effect is seen in these thin film samples, i.e., to first order V is constant with the depth of penetration into the PS layer, all the way down to the substrate.

For 1000k PS in Figure 4, the effects of preannealing were even more exaggerated. Relatively high preannealing temperatures of ~166 °C were needed to reach a limiting value of V. Even at preannealing temperatures tens of degrees above T_g (=106 °C), significant changes in V are observed. For 20000k PS in Figure 5, significant variations in V are seen even after 30-min exposures at preannealling temperatures of 177 °C. Even at this temperature, this very high MW PS is still not completely relaxed. Higher preannealling temperatures were not attempted because of concerns of degrading the polymer in our N_2 purged oven.

V for the four PS MWs are summarized vs preannealing temperature in Figure 6. For 10k PS, there is only a slight difference between samples preannealed above and below T_g (=99 °C). For 100k and 1000k PS, V reaches limiting values at preannealing temperatures of ~120 and 160 °C, respectively. It is clear from Figure 6 that 20000k PS is

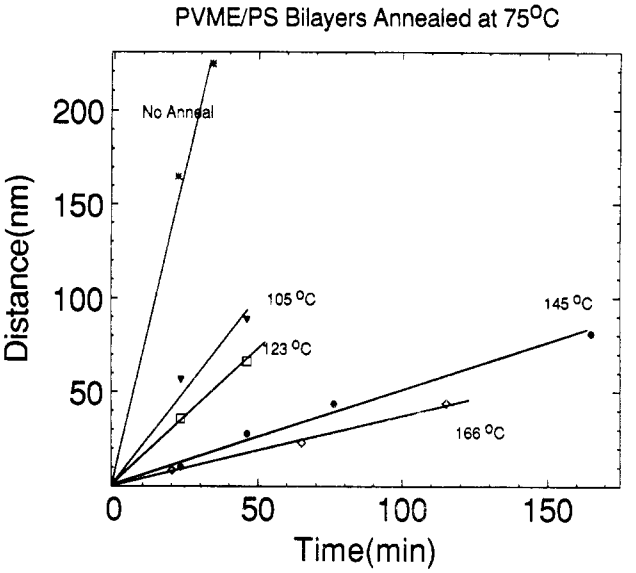

Figure 4. Decrease in 1000k PS layer thickness at interdiffusion temperatures of 75 °C. 30-min preanneals (in N_2) of the PS layers were applied at the indicated temperatures.

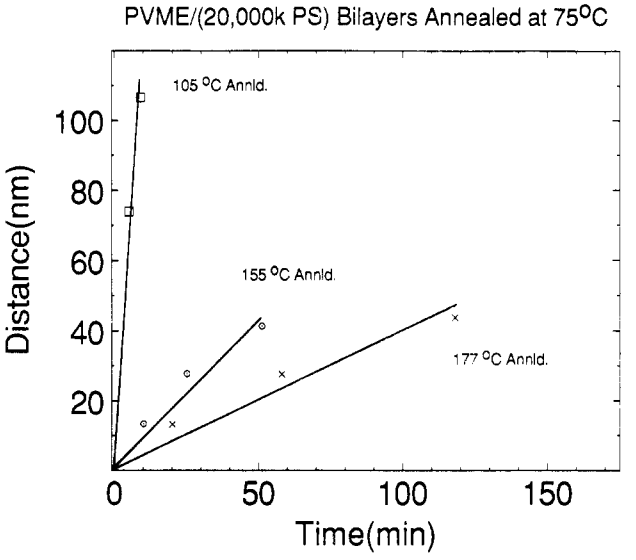

Figure 5. Decrease in 20000k PS layer thickness at interdiffusion temperatures of 75 °C. 30-min preanneals (in N_2) of the PS layers were applied at the indicated temperatures.

far from reaching its limiting value, even at 177 °C.

Instead of our standard 30-min annealing times, we found that longer anneals at lower temperatures could be used, resulting in a similar effect. An example is shown in Figure 7, where 1000k PS samples were preannealed at 123 °C for different times up to 960 min. Plotting log V versus log time gives a relatively straight line (inset, Figure 7). The solid point is calculated by the reptation model, as will be discussed later.

The 75 °C interdiffusion data for PS films are shown in Figure 8. The front velocities are comparable for 1000k and 20000k because the latter was not completely relaxed. The 10k, 100k, and 1000k data correspond to fully relaxed films. There is some variation of V with MW (inset, Figure 8), but not as strong as the well-known M^{-2} dependence for Fickian diffusion of polymers above their entanglement molecular weight. The 20000k PS data are not included on this plot because this PS was not fully relaxed. In the case of low MW penetrants, case II front velocities are relatively independent of the polymer glass MW because dissolution of the polymer is not a factor, only mechanical relaxations and local friction effects. Thus, the MW

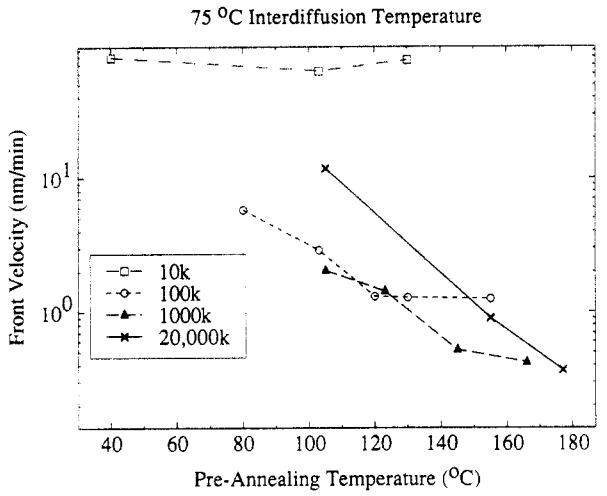

Figure 6. Front velocity (V) vs. the preannealing temperature for the different PS MWs indicated. (See text.)

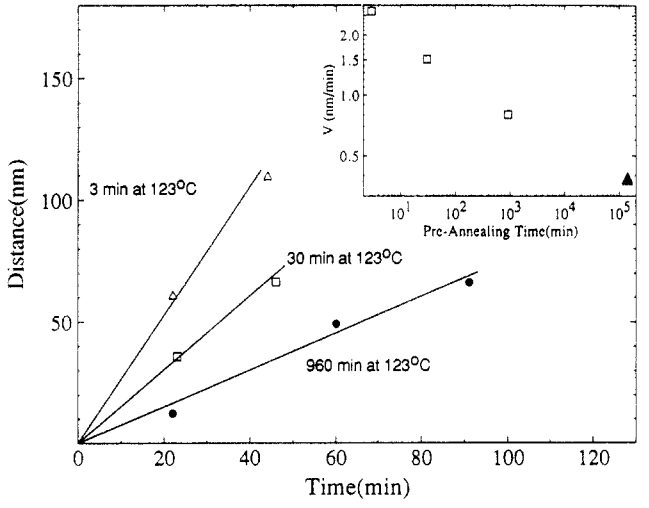

Figure 7. Effect of preannealing of 1000k PS at 3, 30, and 960 min at 123 °C on interdiffusion at 75 °C. Inset: log of front velocity (V) versus log of preannealing time. The open points are experimentally determined, and the solid point is calculated using the reptation model (see text).

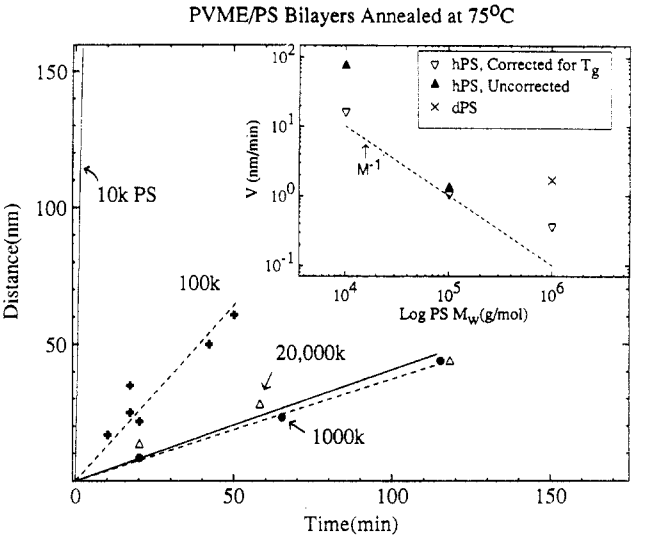

Figure 8. Interdiffusion at 75 °C for fully relaxed PS films of the indicated molecular weights. The front velocities are comparable for 1000k and 20000k because the latter was not completely relaxed. Inset: Dependence of V on PS MW for interdiffusion temperatures of 75 °C. One point for a 1000k deuterated PS(dPS) sample is also included. T_g's are 99, 105, and 105.6 °C for 10k, 100k and 1000k, respectively. The temperature dependence of V allows one to calculate corrected values of V, considering the difference between the T_g's and 75 °C. These are shown in the inset as the open triangles.

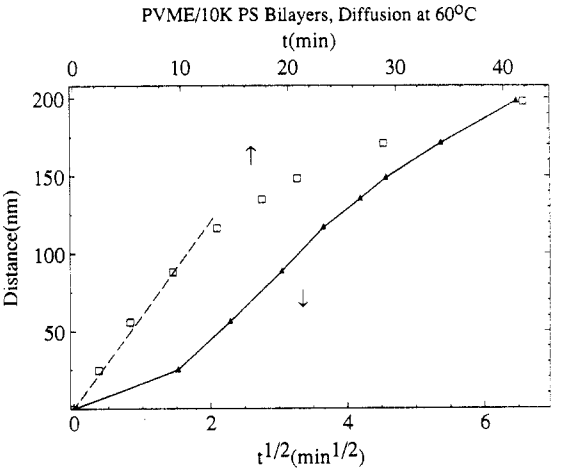

Figure 9. Decrease in 10k PS layer thicknesses versus t^1 and $t^{1/2}$ at interdiffusion temperatures of 60 °C. (See text.)

dependence for PS/PVME (inset, Figure 8) is somewhere between Fickian diffusion and classical case II transport.

An additional factor not easily accounted for in terms of modeling is the enhanced driving force due to the increased miscibility of low MW PS with PVME compared to high MW PS. This could contribute to part of the observed variation in V with PS MW. The depressed coexistence curve (lower critical solution temperature) of high MW PS compared to low MW PS is evidence of the increased miscibility of the latter.[19] We also find experimentally that there is almost 1 order of magnitude difference between 1000k deuterated PS and 1000k hydrogenated PS (inset, Figure 8), which is also explained in terms of an increased driving force for dPS. The depressed coexistence curve of hPS/PVME compared to dPS/PVME is again the experimental evidence[20] of the enhanced miscibility of the latter pair.

Low Temperature Interdiffusion, 10k PS. Data for 10k PS bilayers annealed at 60 °C are shown in order to illustrate typical effects at later stages of interdiffusion (Figure 9). There is a linear behavior at short times and a slowing down at later times. The data in Figure 9 are another example of the fact that the $t^{1/2}$ Fickian dependence does not hold at any stage of the process. The slowing down at longer times is due to an increase in PS concentration in the PVME layer. For example, Figure 9 and Table 2 indicate that after 42 min, about 200 nm of PS has been dissolved, corresponding to an increase in the PVME layer thickness to 450 nm. Thus, the PVME layer is diluted to ~55% PVME after 42 min (Table 2), reducing mobility because of the increase in T_g from −31 to ~+25 °C. The dilution by PS also decreases the driving force for PVME penetration, and both of these contribute to the slowing down at later times. Table 2 also indicates that at all stages the interface stays sharp because of rapid dissolution of 10k PS from the interface region into the PVME phase.

With 10k PS, we were also surprised to find that interdiffusion occurred at room temperature (Figure 10), but at transport rates approximately 4 orders of magnitude slower than those at 75 °C (Figure 11). We suspected that this slow interdiffusion process could be quite sensitive to various features such as PVME polydispersity or incomplete relaxation effects of the PS layer. Data for the fractionated PVME, along with the standard PVME, are

Table 2. Layer Thicknesses and Compostions for Interdiffusion at 60 °C, PVME (100k)/PS (10k)

time, min	thickness, nm PVME	interface[a]	PS	χ^3
0	255 (100% PVME[b])	10	489	0.0058
2.3	282 (93% PVME[b])	8	464	0.0090
5.2	314 (82% PVME[b])	5	433	0.0046
9.2	345 (76% PVME[b])	6	401	0.0055
13.3	374 (71% PVME[b])	5	373	0.0083
17.5	396 (69% PVME[b])	5	354	0.0099
20.8	407 (66% PVME[b])	5	341	0.0078
28.8	427 (62% PVME[b])	5	318	0.0049
41.8	452 (55% PVME[b])	5	291	0.0069

[a] The interface is assumed to be a block with a composition that is the average between the PS and the PVME phase compositions. It is roughly equivalent to a linear gradient interface. [b] Determination of the refractive index of the PVME "layer" by ellipsometry gives these compositions.

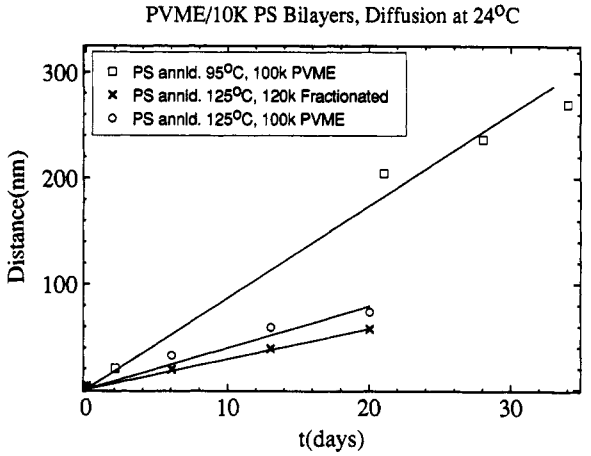

Figure 10. Room temperature interdiffusion of 10k PS/PVME bilayers. V is larger as a result of a 95 °C preanneal of the PS layer (see text). The decreased polydispersity in the reprecipitated 120k PVME had no effect on the interdiffusion rate in the 125 °C preannealed PS films.

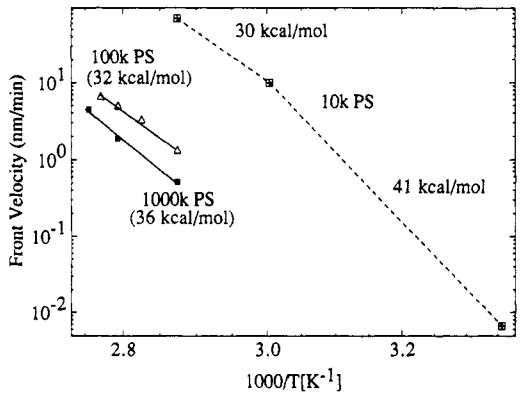

Figure 11. Arrhenius plot of the front velocity for the different PS molecular weights indicated. Fully preannealed PS layers were used in all cases. (See text.)

shown in Figure 10. The polydispersity of the PVME has no measurable effect on V at 24 °C, as was found previously[6] for other interdiffusion conditions. Figure 10 also shows data for a PS layer preannealed at 95 °C. This is enough to remove the xylene, but there is about a factor of 2 increase in V, possibly due to incomplete relaxation of the PS layer or physical aging of the PS.[21] It should be noted that incomplete relaxation effects had almost no effect on higher temperature (75 °C) interdiffusion rates for 10k PS, as was shown in Figure 6.

Arrhenius Plots. A typical plot of the raw data for a fully relaxed 1000k PS film as a function of interdiffusion

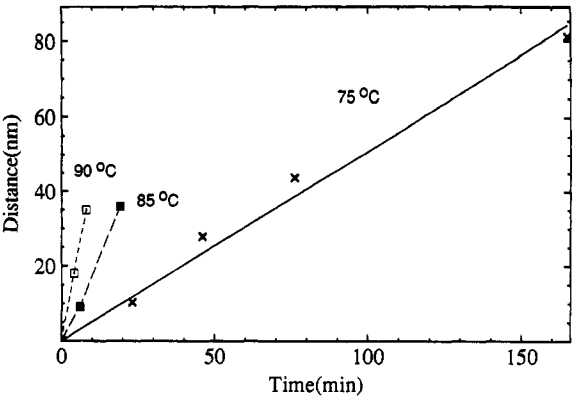

Figure 12. Temperature dependence of PVME interdiffusion for fully preannealed 1000k PS films.

temperature is shown in Figure 12. The Arrhenius plots are given in Figure 11 where all PS films were fully relaxed. The data for 100k and 1000k PS are mostly concentrated in the region between 90 and 75 °C. The apparent activation energies (E_a) are generally between 30 and 40 kcal/mol, which convert to E_a/RT values ranging from 43 to 57, respectively where R = 0.001 98 kcal mol^{-1} K^{-1}. We have found that incompletely relaxed PS films lead to comparable values of E_a, although the absolute values of V are different. The high values are comparable to those determined by methanol/PMMA at room temperature, E_a/RT = 42, and are typical of case II diffusion for many systems.[11,12] The values are much higher than those obtained for Fickian diffusion, which generally fall in the range of E_a/RT = 20 depending on the proximity to the polymer T_g. The high values of E_a are indicative of the importance of cooperative mechanical relaxation effects in the boundary of the unswollen glass and partially swollen PS/PVME front region. They are comparable to those values of E_a obtained for cooperative relaxations such as creep in polymer glasses.[12]

Preliminary data for the temperature dependence of 10k PS indicate some departure from Arrhenius behavior (Figure 11). For example, E_a is seen to decrease slightly at higher temperatures of 75 °C. Mechanical relaxation effects in the glass would be less dominant as one approaches T_g because of the softening of the glass. Also, at temperatures above T_g (=99 °C for 10k PS), one must approach a Fickian diffusion regime governed by lower activation energies. The apparent activation energies for viscosity and diffusion of PS, PVME, and blends have been reviewed recently.[22,23]

Discussion

Asymmetric Interfacial Profiles. In the case of incompletely relaxed PS layers, it was found that both higher PS molecular weights and higher interdiffusion temperatures accentuated the asymmetric interfaces. This interface consists of a low PVME volume fraction penetration front which extends into the PS layer (inset, Figure 2). This front is about 40 nm for 100k PS[6] and increases to 80 nm for 1000k PS (Table 1) for comparable interdiffusion conditions. To a first approximation, the magnitude of the PVME front velocity, relative to the PS swelling and dissolution rate into the PVME phase, is the main factor in determining the extent of the asymmetric profile buildup. Only with solvent penetration of polymer glasses can one reach the limiting case where negligible polymer dissolution occurs, and a low volume fraction solvent front extends through the entire glass.[12] The PVME penetration front was never observed to extend

indefinitely into the PS layer, but with high MW PS, dissolution becomes significantly slower. In these cases where the PVME front velocity is relatively rapid, asymmetric profiles can be generated as was shown in the inset of Figure 2. The other limiting case is seen with low MW PS (e.g., 10k), where the PS dissolution rate is very fast compared to the front velocity. For example, Table 2 indicates that the interface remains narrow (~5 nm) and symmetric as the PVME dissolves the PS in an etching type of process.

If one considers interdiffusion temperatures in the range ~60–85 °C, it is found that for the higher temperatures the asymmetric profiles can be accentuated. The front velocity is highly coupled to the PS mechanical relaxation rate,[6] which varies rapidly with temperature in this region just below T_g. Because of the low T_g of PVME, the mobility of the PVME phase is only varying slowly in this temperature region. As a result of this, the mismatch is exaggerated between the PS dissolution rate and the front velocity as one approaches ~85 °C, giving rise to the broader asymmetric profile.

In the course of this study it was found that it was much more difficult to generate the asymmetric profiles discussed above for "completely relaxed" PS films, i.e., single PS films preannealed at $T \gg T_g$. This is mainly because the PVME front velocity is slowed significantly in cases of completely relaxed PS films. Since the occurrence of asymmetric profiles in these type of systems was one of the features that led us to suggest that there were some similarities of PVME/PS transport[6] to classical case II solvent transport,[12] this development sheds some doubt on any quantitative similarities between the two types of systems.

Relaxation of PS Entanglement Density in Solvent Cast Films. A major complication was discovered as we attempted to extend the original studies to other PS MWs. We were concerned at first that the interdiffusion rates (front velocities) were not very reproducible, with the lack of reproducibility exaggerated at higher PS MWs. After much effort, the problem was traced to the temperature at which melt preannealing was applied to the single PS layer. The preannealing was originally applied simply to remove xylene, which was the PS spinning solvent, and to relax orientation. The preannealing temperature was above the PS T_g, but varied between 105 and 120 °C in the first several experiments where irreproducibility was detected. The difference was enough to change the transport rate (front velocity, V) of PVME into 100k and 1000k PS by a few hundred percent. After discovering the importance of this, the preannealing temperature was controlled to within a few degrees and the old data were discarded. Figures 3–5 illustrate this remarkable preannealing effect on V for the different PS MWs once this effect was controlled.

In an attempt to understand the cause of the variation of V with the PS preannealing temperature, effects of degradation or oxidation of PS were initially investigated. Experiments showed that preannealing the PS films at 150 °C in air gave results identical to those for preannealing in N_2. As was discussed above, the value of V was constant with the depth of PVME penetration into the PS layer. This lack of a skin effect was further indication that oxidation was not a factor. Solvent retention in the PS films was ruled out because the diffusion rate at $T > T_g$ should be independent of PS molecular weight for the MWs in question. Also, solvent mobility close to the PS T_g should be very high and removal should be rapid considering the high surface to volume ratio of the films.

Table 3. Relaxation of Birefringence[a] as a Function of Annealing Temperature in 900-nm-Thick Spin Coated 1000k PS Films

	before anneal	after anneal (103 °C, 30 min)
TE	1.5776	1.5779
TM	1.5803	1.5764
	before anneal	**after anneal (145 °C , 90 min)**
TE	1.5773	1.5772
TM	1.5798	1.5755

[a] The precision in refractive indices was better than ±0.0003. The accuracy is better than 0.001.

Physical aging, which is a densification of polymers which occurs during annealing below T_g, is known to effect case II solvent transport.[21,24] In PVME/PS we do not observe any significant effect of physical aging. For example, the PVME front velocity for a PS single layer physically aged at 85 °C for 3 days was identical to that for a PS film which was physically aged under the same conditions, but the aging was erased by melt annealing the film above T_g and quenching. Many of the other features discussed below indicate that physical aging has a negligible effect under our experimental conditions.

Birefringence and Internal Stress in Solvent Cast PS Films. The next logical step was to investigate the influence of internal stress in the solvent cast films, as possible driving forces for accelerated interdiffusion. Drying stresses[25] during the late stages of solvent evaporation lead to substantial orientation which is manifested as a measurable film birefringence. The internal stress of ~1 MPa[26] associated with orientation would be a possible contribution to the driving force[27] for interdiffusion of PS and PVME, if it persisted under our preannealing conditions. It was shown previously[25] with solvent cast films, that birefringence was removed by annealing at the T_g (~105 °C) of high MW PS. For our spin coated 1000k PS films, annealing at 103 °C also removes the birefringence (difference between TM and TE refractive indices approaches zero in Table 3), as does annealing at temperatures well above T_g, as was expected. For this PS MW, incomplete relaxation effects were seen in the measured V up to preannealing temperatures of ~150 °C (Figure 4). Thus, orientation is certainly not a factor in explaining the effects which persist even after PS films were preannealed well above T_g (Figures 3–6). It is reasonable that relaxation of orientation in the melt would occur far more rapidly than center of mass diffusion, since the former is a shorter length scale relaxation.

Evidence for Incomplete Entanglement Density in PS Layers. Graessley[28] has shown that the MW between entanglements (M_e) is inversely proportional to the polymer weight fraction in solution:

$$M_e^{soln} \sim M_e^{melt}/\phi \quad (1)$$

where M_e^{soln} is the MW between entanglements in solution, M_e^{melt} is the MW between entanglements in the melt, and ϕ is the polymer weight fraction. For a 1% solution, which is typical for spin coating high MW PS, the entanglement density is reduced by 2 orders of magnitude! The mechanical consequences of the reduced entanglement state have been documented for solution cast films of polyethylene.[29] With the very high molecular weights, at least some of the "dilute" solution characteristics, in terms of a reduced entanglement density, are detected in the solidified film.[29] In our PS films, which are also spin coated from relatively dilute solutions at 25 °C, the chains collapse in a less entangled state[29,30] and are frozen in this state because of rapid solvent removal. This quenching in of

Table 4. Longest Relaxation Times (τ_t, in Minutes) in PS Melts Calculated by the Reptation Model

M_w	103 °C	120 °C	145 °C	170 °C
10k[a]	2.4×10^2	2.4×10^{-1}	1.2×10^{-3}	7.9×10^{-5}
100k		2.4×10^2	1.2×10^0	7.9×10^{-2}
1000k		2.4×10^5	1.2×10^3	7.9×10^1
20000k		1.9×10^9	1.0×10^7	6.3×10^5

[a] This is below the PS entanglement MW, so the predicted value of τ_t is too high and is an upper limit.

an unentangled state should be more pronounced for high MWs because of the extended relaxation times, even in solution. Also, to get similar layer thicknesses with comparable spinning speeds, the high MW PS solutions are made much more dilute than the low MW solutions.

The evidence suggests that melt preannealing at $T \gg T_g$ is required to attain an equilibrium entanglement density and that equilibration is necessary to reach a limiting value of V. Because the relaxation times increase substantially in the melt with higher MWs, the preannealing temperature at which the limiting values of V are reached are significantly higher for high MWs, i.e., ~120 °C for 100k PS compared to ~160 °C for 1000k (Figures 3 and 4). The rate of reentanglement should be related to the rate of center of mass diffusion. To make quantitative comparisons, the reptation or longest relaxation time (τ_t) is calculated using the reptation model:[31]

$$D_{rep} \approx Na^2/\tau_t \approx D_1 N^{-2} \quad (2)$$

where D_{rep} is the polymer self-diffusion coefficient, N is the degree of polymerization, a is the effective segment length (~6.7 Å for PS), and D_1 is the monomer friction factor. D_1 was obtained by normalizing with a literature value for D_{rep} which was measured to be 0.9×10^{-18} m²/s for 1000k PS at 170 °C.[32] The temperature dependence was obtained by assuming that D_1 scales with the PS zero shear viscosity,[23,33] which is highly non-Arrhenius over the temperature region from the melt down to the glass transition. Predictions of the longest relaxation times τ_t are given in Table 4 for the four MWs studied. For the standard annealing time of 30 min, the temperatures at which plateau values in V are seen for 100k and 1000k PS are slightly higher but qualitatively consistent with the temperature at which τ_t is predicted to be about 30 min (Table 4). PS (10k) is predicted to reach an equilibrium entanglement density simply by annealing very close to T_g, consistent with the observed trend in the values of V for this MW (Figure 6). The predictions also indicate that 630 000 min at 170 °C is necessary for 20000k PS! This explains why there is almost no change in slope in Figure 6 for 20000k, after 30-min preanneals of 177 °C. At temperatures of 230 °C, τ_t is still predicted to be several weeks for 20000k PS< so we did not attempt any extended anneals at such high temperatures because of the possibility of degradation.

In terms of the 123 °C annealing experiments in Figure 7, the reptation prediction for 1000k PS at this temperature is 140 000 min. This is used with the experimentally determined limiting value of V = 0.38 nm/min for fully relaxed 1000k PS films from Figure 6, resulting in the solid triangle in the inset of Figure 7. The observed trend is consistent with the other measured values in the inset of Figure 7, which is further evidence for a reptation type of process governing the rate to an equilibration entanglement density in the PS melt.

Conclusions

Interdiffusion of 100k PVME and PS (10k, 100k, 1000k, and 20000k) was monitored at temperatures below the glass transition of PS. The transport of PVME into PS under these conditions was highly non-Fickian, and a linear dependence with time was found. Some similarities to classical case II transport of solvent into polymer glasses are seen such as the non-Fickian transport and high apparent activation energies. Unlike case II solvent transport, the MW of the polystyrene influences the PVME front velocity because of MW dependence of the rate at which the PS can be swollen and dissolved. Because PS dissolution occurs during PVME transport into glassy PS, in many cases no asymmetric front is observed.

It was also found that the front velocity of PVME into PS depended strongly on the temperature and time of "pre-annealing" of the single spin coated PS layer, with incompletely preannealed PS films leading to order of magnitude increases in front velocities. For higher MW PS, preannealing at temperatures well above T_g was necessary to reach a plateau value in front velocity consistent with a molecular relaxation phenomena. Orientation, degradation, and solvent retention were ruled out by various control experiments. The results indicate solvent casting of high MW PS freezes in a reduced entanglement state which is known to exist in solution,[28] leading to a marked increase in PVME front velocities. The MW dependence of PS reentanglement obtained by melt annealing at $T \gg T_g$ can be qualitatively modeled in terms of the longest relaxation time calculated with the reptation model. The reduced entanglement state is expected to be a general feature of all high MW, solvent cast polymer films and could be an important factor in a variety of interdiffusion studies.

Acknowledgment. We thank G. P. Felcher, W. Dozier, R. Goyette, S. R. Lustig, Y. Termonia, J. Van Alsten, M. Rafailovich, J. Sokolov, and R. Briber for their contributions. The work at the Argonne facility was funded by DOE, BES-Materials Science, under Contract W-31-109-Eng-38.

References and Notes

(1) Kawaguchi, M.; Miyake, E.; Kato, T.; Takahashi, A. *Kobunshi Ronbunshu* **1981**, *38*, 341.
(2) Yukioka, S.; Inoue, T. *Polym. Commun.* **1991**, *32*, 17.
(3) Yukioka, S.; Nagato, K.; Inoue, T. *Polymer* **1992**, *33*, 1171.
(4) Arwin, H.; Aspnes, D. E. *Thin Solid Films* **1986**, *138*, 195.
(5) Walsh, D. J.; Sauer, B. B.; Higgins, J. S.; Fernandez, M. L. *Polym. Eng. Sci.* **1990**, *30*, 1085.
(6) Sauer, B. B.; Walsh, D. J. *Macromolecules* **1991**, *24*, 5948.
(7) Russell, T. P. *Mater. Sci. Rep.* **1990**, *5*, 171.
(8) Jabbari, E.; Peppas, N. A. *Macromolecules* **1993**, *26*, 2175.
(9) Deppe, D.; Spangler, L.; Torkelson, J. *Polym. Prepr. Am. Chem. Soc., Div. Polym. Chem.* **1993**, *34* (2), 502.
(10) Composto, R. J.; Kramer, E. J. *J. Mater. Sci.* **1991**, *26*, 2815.
(11) Hopfenberg, H. B.; Frisch, H. L. *Polym. Lett.* **1969**, *7*, 405.
(12) Windle, A. H. In *Polymer Permeability*; Comyn, J., Ed.; Elsevier: London, 1985; p 75.
(13) Mills, P. J.; Kramer, E. J. *J. Mater. Sci.* **1986**, *21*, 4151.
(14) Brochard, F.; de Gennes, P.-G. *Physicochem. Hydrodynam.* **1983**, *4*, 313.
(15) Herman, M. F.; Edwards, S. F. *Macromolecules* **1990**, *23*, 3662.
(16) Lustig, S. R.; Caruthers, J. M.; Peppas, N. A. *Chem. Eng. Sci.* **1993**, *47*, 3037.
(17) Lustig, S. R. Ph.D. Thesis, Purdue University, 1989. Kim, D.-H.; Caruthers, J. M.; Peppas, N. A. Submitted for publication to *Chem. Eng. Sci.*
(18) Anastasiadis, S. H.; Russell, T. P.; Satija, S. K.; Majkrzak, C. D. *J. Chem. Phys.* **1990**, *92*, 5677.
(19) Nishi, T.; Wang, T. T.; Kwei, T. K. *Macromolecules* **1975**, *8*, 227.
(20) Ben Cheikh Larbi, F.; Leloup, S.; Halary, J. L.; Monnerie, L. *Polym. Commun.* **1986**, *27*, 23.
(21) Hui, C.-Y.; Wu, K.-C.; Laskey, R. C.; Kramer, E. J. *J. Appl. Phys.* **1987**, *61*, 5129.

(22) Green, P. F. *Macromolecules* **1991**, *24*, 3373.
(23) Green, P. F.; Adolf, D. B.; Gilliom, L. R. *Macromolecules* **1991**, *24*, 3377.
(24) Lasky, R. C.; Kramer, E. J.; Hui, C. Y. *Polymer* **1988**, *29*, 673.
(25) Prest, W. M.; Luca, D. J. *J. Appl. Phys.* **1980**, *51*, 5170.
(26) Prest, W. M.; Luca, D. J. *J. Appl. Phys.* **1979**, *50*, 6067.
(27) More, A. P.; Donald, A. M.; Henderson, A. *Polymer* **1992**, *33*, 3759.
(28) Graessley, W. W. *Adv. Polym. Sci.* **1974**, *16*, 58.
(29) Termonia, Y.; Smith, P. *Macromolecules* **1988**, *21*, 2184.
(30) Grosberg, A. Y.; Nechaev, S. K.; Shakhnovich, E. I. *J. Phys. Fr.* **1988**, *49*, 2095.
(31) de Gennes, P. G. In *Scaling Concepts in Polymer Physics*; Cornell University: Ithaca, NY, 1979.
(32) Green, P. F.; Mills, P. J.; Palmstrøm, C. J.; Mayer, J. W.; Kramer, E. J. *Phys. Rev. Lett.* **1984**, *53*, 2145.
(33) Ferry, J. D. *Viscoelastic Properties of Polymers*; Wiley: New York, 1980.